Journal of the Korean Physical Society, Vol. 36, No. 6, June 2000, pp. 346∼350

Charge Carrier Tunneling in the Light-Emitting Diodes of Poly (p-phenylene) Thin Films

J. W. Jeon, G. W. Kang and C. H. Lee *
Department of Physics, Inha University, Inchon 402-751

W. J. Song and C. Seoul
Department of Textile Engineering, Inha University, Inchon 402-751

(Received 10 November 1999)

We have studied the temperature dependence of the current-voltage (I-V) and the electroluminescence-voltage (EL-V) characteristics in the blue light-emitting diodes of vacuum-deposited poly (p-phenylene) (PPP) thin films in the temperature range between 14 and 290 K. The onset of the EL occurs at an electric field of about 7×10^7 V/m, independent of the thickness of the PPP layer. The I-V and EL-V dependences show very weak temperature dependences and fit very well with the Fowler-Nordheim tunneling formula. The results suggest that charge carrier injection is a tunneling process through an energy barrier of about 0.6∼0.8 eV in indium tin oxide (ITO)/PPP/Al devices.

I. INTRODUCTION

The development of the π-conjugated polymers as electronic materials has attracted increasing scientific and technological interests [1–3]. The nonlinear excitations such as solitons, polarons, and bipolarons which are formed due to a strong electron-phonon interaction in the π-conjugated polymers have been intensively studied to understand the various physical properties [1–7]. Among many potential applications of the π-conjugated polymers, electroluminescence (EL) devices have become very attractive for their applications in large-area, full-color, flat-panel displays and organic laser diodes [1,2]. Since Tang and Van Slyke at Kodak [8] firstly reported thin-film multilayer organic light-emitting diodes (LED) with a high luminous efficiency at low voltage, there has been significant improvement in their performance and stability. For example, the maximum luminous efficiency of ∼22 lm/W, recently reported for a green polymeric LED, is comparable to that of inorganic semiconductor LEDs [2]. In addition, their emission spectra span the whole gamut of the visible spectral region. These results clearly demonstrate the great potential of the organic LED technology as a next-generation display technology. It is, therefore, very important to attain a comprehensive understanding of the operating mechanism of the organic LED to further improve this technology.

One of important issues is an understanding of the mechanism that controls the current flow in the organic LED [1,2]. The current flow of the organic LED is determined by the injection, the transport, and the recombination of charge carriers. I. D. Parker [9] showed that charge injection is limited by tunneling through the energy barrier at the interfaces between the polymer layer and the anode or the cathode. The smallest energy barrier at either interface determines the injection rate of the majority carrier [9]. The smaller measured current compared with the calculated tunneling current is explained as the result of a large backflow of injected carriers into the injecting electrode due to the low mobility typical of organic semiconductors [10]. Then, the net device current is the injected current minus the backflow current [10]. Measurements of internal electric fields showed that the energy barriers for electron or hole injection depend on the difference between the electrode work function and the lowest-unoccupied-molecular-orbital (LUMO) or the highest-occupied-molecular-orbital (HOMO) [11]. However, there are many reports that current flow in diodes with low barriers is bulk-limited through the buildup of space charges in organic semiconductors with a distribution of traps [12–14].

In general, the processes of charge carrier injection from electrodes and the carrier transport within the organic layers are difficult to separate from the electrical characteristics of the device. However, we can determine the dominant mechanism limiting the current through a systematic study of the current-voltage (I-V) dependence on the temperature and the film thickness since the

*E-mail: chlee7@inha.ac.kr, Fax: +82-32-872-7562

tunneling injection and the space-charge-limited-current (SCLC) models predict different *I-V* dependence.

The tunneling mechanism for charge injection predicts that the current is temperature independent and depends on the electric field [9]. The Fowler-Nordheim (FN) tunneling model predicts that at large forward bias the current is given by

$$I \propto F^2 e^{-\frac{\kappa}{F}} \quad (1)$$

where F is the electric field strength and κ is a parameter that depends on the barrier shape [9]. If the injected charge is assumed to be tunneling through a triangular barrier, the constant κ in Eq. (1) is given by

$$\kappa = \frac{8\pi(2m^*)^{\frac{1}{2}}\varphi^{\frac{3}{2}}}{3qh} \quad (2)$$

where φ is the Schottky energy barrier, m^* is the effective mass of the charge carriers, q is the magnitude of the electronic charge, and h is Planck's constant [9]. The SCLC model predict a power-law dependence of the current on the voltage and the thickness d with the exponent m varying with the temperature T:

$$I \propto \frac{V^{m+1}}{d^{2m+1}}, \quad (3)$$

$$m = \frac{E_t}{k_B T}, \quad (4)$$

where k_B is Boltzmann's constant and E_t is the characteristic trap energy of the exponential trap distribution in the band gap [15].

Recently, PPP-based oligomers and polymers have gained significant interest because of their high luminescence efficiency in the blue spectral range and good thermal stability [16]. However, it is infusible and insoluble so that it is not easy to use to fabricate a thin film. Thus, the vacuum deposition of PPP thin film has been investigated by several groups [17,18]. In this research, we studied the *I-V* dependence on the temperature T and the film thickness d to clarify the operating mechanism for the current limitation in blue-emitting LEDs fabricated with vacuum-deposited poly (*p*-phenylene) (PPP) thin films [19,20]. The charge carrier injection is found to be a tunneling process through an energy barrier of about 0.6∼0.8 eV in ITO/PPP/Al.

II. EXPERIMENT

The details of the synthesis and the characterization of the PPP used in this study were reported elsewhere [20]. The phenylene chain length can be calculated from the IR peak intensity ratio of the para-band (800–830 cm^{-1}) to the mono-substituted phenylene ring band (690–710 cm^{-1}) [17]. The IR spectrum analysis showed that the average phenylene chain lengths of the parent PPP powder and the vacuum-deposited PPP thin film were about n=27–28 and n=8–9, respectively [19,20]. It was reported that the molecular weight decrease in vacuum-deposited PPP films compared with PPP synthesized with chemical polymerization [17,18].

Indium tin oxide (ITO) glass with a sheet resistance of about 10 Ω/□, supplied by Samsung Corning Co., Ltd., was cleaned in ultrasonic baths of toluene, isopropyl alcohol, acetone, and methanol, respectively, and then loaded into a vacuum-deposition chamber. The PPP thin film was deposited onto the ITO substrate by heating the PPP powder to 500 °C under a vacuum of about 2×10^{-6} Torr. The thickness of the PPP layer was varied from 120 to 710 nm. The Al electrode with an active area (the overlap of ITO and Al) of about 4 mm^2 was vacuum- deposited on top of the PPP layer.

The devices were mounted on to the cold finger of cryostat under vacuum. The *I-V* characteristics were measured in the temperature range between 14 and 290 K with a Keithley 2400 source meter. The intensity of the EL emission from the devices was simultaneously measured with a Keithley 2000 multimeter equipped with a calibrated Si photodiode or an ARC P2 PMT through an ARC 275 monochromator. The external EL quantum efficiency (QE), the ratio of the emitted photons to the injected charges, was calculated from the luminous output measured by the calibrated Si photodiode. The *I-V-L* characteristics were studied in the temperature range between 14 and 300 K. The EL and PL spectra were measured with a spectrofluorophotometer (Shimadzu RF-540). The absorption spectra of PPP thin films deposited onto quartz substrates were measured with a UV-Vis spectrophotometer (Scinco S-2140).

III. RESULTS AND DISCUSSION

Figure 1 show the (a) *I-V* and the (b) *EL-V* characteristics of ITO/PPP/Al devices with different PPP thicknesses (d=120, 260, 360, 650, and 710 nm) at T=290 K. The devices exhibit rectifying *I-V* characteristics with a blue EL emission (peak at 446 nm) [19]. The forward bias is defined as the positive bias on the ITO electrode. The device with a film thickness of d=120 nm shows a noisy current at low voltage due to the leakage current, arising from pinholes in the PPP thin film. We found that the EL intensity increased linearly with the current in all devices and that the slope of the *EL-I* curves was proportional to the external quantum efficiency of the EL. The ITO/PPP/Al devices showed an external quantum efficiency of about 0.02 % [19].

Figure 1(a) clearly shows that reducing the PPP film thickness lowers the operating voltage of the device. Figure 2 displays the current data in Fig. 1(a) as a function of the applied electric field $F = V/d$ and indicates that the current depends on the electric field not on the applied voltage over a wide range of device thickness

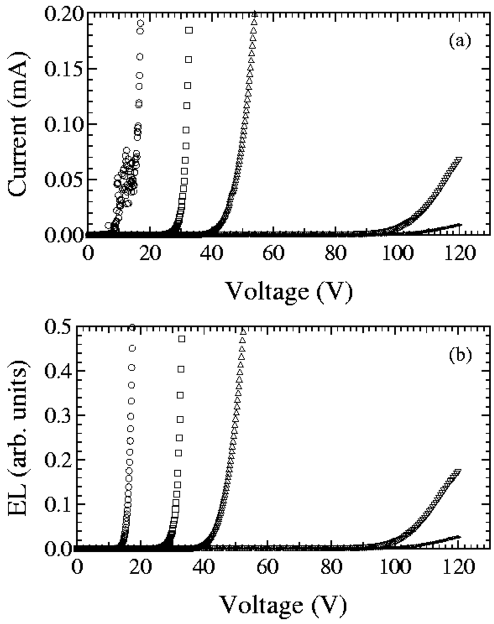

Fig. 1. The forward biased (a) I-V and (b) EL-V characteristics of the ITO/PPP/Al devices with various PPP thicknesses, d=120 (◯), 260 (□), 360 (△), 650 (▽), and 710 nm (◇), at T=290 K.

(d=120∼710 nm). It is found that the onset of EL occurs at an electric field strength of about 7×10^7 V/m, independent of the thickness of the PPP layer. The results suggest a tunneling model for carrier injection in which one, or both, of the carriers is injected through an energy barrier at the electrode/PPP interface under the applied field.

Figure 3 shows the Fowler-Nordheim plot, ln (I/F^2) vs $1/F$, of the data in Fig. 2. As expected, the plot is very close to linear at high field, indicating tunneling [9]. The deviation from linearity at high voltage is due to the series resistance of the device and degradation of the device arising from Joule heating and that at lower field was thought to be due to a thermionic emission contribution to the current [9,10]. The I-V and the EL-V characteristics of LEDs with structures of poly (p-phenylenevinylene) (PPV) derivatives were also reported to fit well to the FN tunneling formula [5,9]. The barrier height can be obtained from the FN fit to the data at high field by using Eqs. (1) and (2). To obtain the zero-field barrier φ_0, we must include the lowering of the potential barrier due to the Schottky effect [15,21]. The

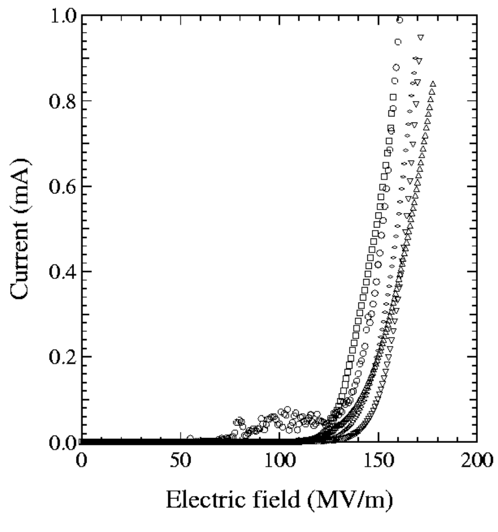

Fig. 2. The current vs electric field $F = V/d$ for the data in Fig. 1 (a) over a wide range device thicknesses (d=120 ∼ 710 nm).

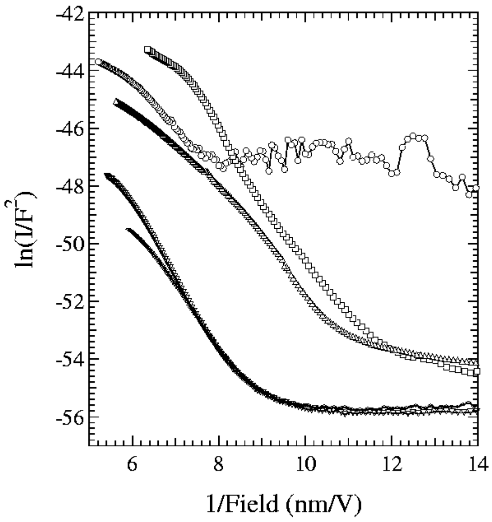

Fig. 3. The Fowler-Nordheim plot, ln (I/F^2) vs $1/F$, of the data in Fig. 2.

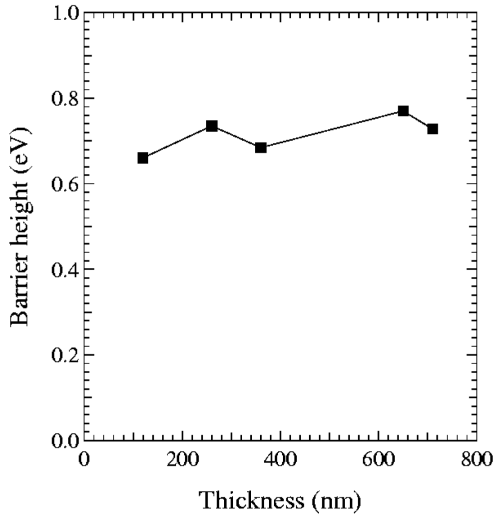

Fig. 4. The zero-field barrier φ_0, calculated from the FN analysis of the data in Fig. 3 by using Eqs. (1)-(3). φ_0 =0.6∼0.8 eV for all ITO/PPP/Al devices with differing PPP thicknesses.

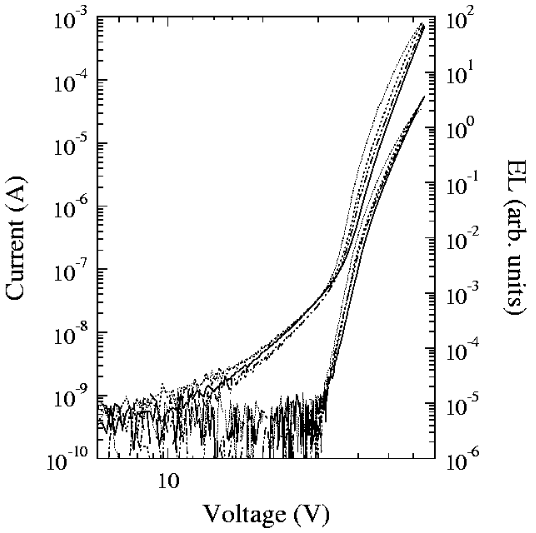

Fig. 5. The current (top 4 curves) and the EL intensity (bottom 4 curves) under a forward bias, on a log-log plot, of the ITO/PPP (d=360 nm)/Al device at temperatures, from top to bottom, T=290, 240, 120, and 14 K.

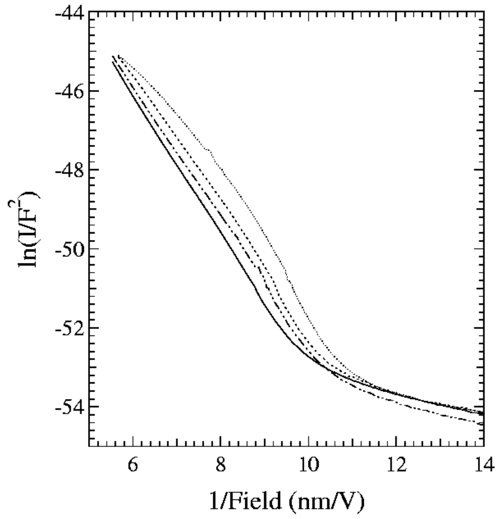

Fig. 6. The Fowler-Nordheim plot of the data in Fig. 5.

effective potential barrier height is field dependent and can be written as

$$\varphi = \varphi_0 - q\sqrt{\frac{q}{4\pi\epsilon}}F^{\frac{1}{2}} \tag{5}$$

where ϵ is the dielectric constant of PPP [15]. Figure 4 shows the zero-field barrier φ_0, calculated from the FN analysis of the data in Fig. 3 by using Eqs. (1)-(3). φ_0 is about 0.6∼0.8 eV for all ITO/PPP/Al devices with differing PPP thicknesses. The HOMO and the LUMO levels were reported as 2.1 and 5.2 eV, respectively, for PPP thin films [18]. Since the work functions of ITO and Al are about 4.7 and 4.3 eV, respectively [9], the measured barrier height of about φ_0=0.6∼0.8 eV is thought to be the energy difference between the ITO work function and the HOMO level of PPP. Thus, the majority carriers are holes injected from the ITO/PPP interface through a tunneling mechanism. We found from the temporal response of the EL upon application of a rectangular voltage pulse that the hole mobility was about 1×10^{-5} cm^2/Vs in vacuum-deposited PPP thin films [22].

It is noted that the current is smaller than the calculated FN tunneling current, although the *I-V* characteristics have a FN functional form. In addition, the current at a given electric field decreases as the film thickness increases. This behavior can be explained as resulting from a backflow of injected carriers into the injecting electrode, as proposed by Davids *et al.* [10]. The buildup of holes at the ITO/PPP interface due to the low mobility of PPP results in a current backflow that becomes more severe in devices with thicker PPP films. The combination of FN tunneling injection and backflow currents establishes a majority carrier (hole) density near the ITO/PPP interface. The device current results primarily from drift of these carriers away from the ITO/PPP contact [10].

Figure 5 shows the temperature dependences of the current and the EL intensity, on a log-log plot, of the ITO/PPP (d=360 nm)/Al device under a forward bias from 290 K down to 14 K. All ITO/PPP/Al devices with different PPP thicknesses showed similar temperature dependence for the *I-V-EL* characteristics. Both the current and the EL intensity show very weak temperature dependences rather than the exponential dependences expected for thermionic emission, again consistent with the tunneling mechanism for carrier injection. Moreover, Fig. 5 clearly indicates that the power-law expected for a SCLC does not fit well the *I-V* and *EL-V* characteristics of the ITO/PPP/Al device. Furthermore, the EL onset voltage remains the same in the temperature range between 14 and 290 K, consistent with the tunneling mechanism, but inconsistent with the SCLC mechanism.

Figure 6 shows the FN plot of the data of Fig. 5 for various temperatures. Again, the good linearity of the FN plot for all temperatures is clearly observed at high field. We can calculate the zero-field barrier φ_0 from the FN analysis by using Eqs. (1)-(3). Figure 7 shows that φ_0 is about 0.7 eV at all temperatures for the ITO/PPP (d=360 nm)/Al device, as expected for tunneling injection. The interesting thing is that this threshold bias voltage is very close to that for light emission.

IV. CONCLUSIONS

We have presented a comprehensive study of the *I-V* and the *EL-V* dependences on the temperature T and the film thickness d to clarify the operating mechanism of current limitation in blue LEDs fabricated with

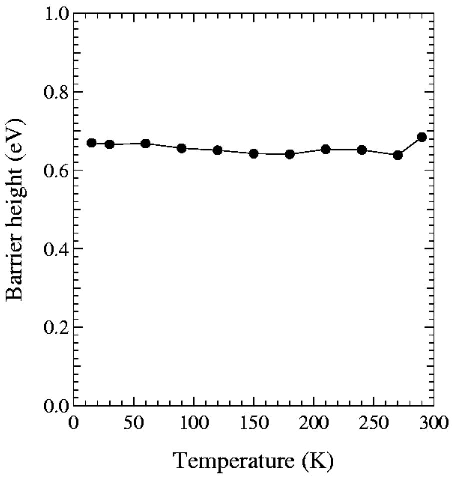

Fig. 7. The zero-field barrier φ_0, calculated from the FN analysis of the data in Fig. 6. $\varphi_0 = 0.7$ eV at all temperatures for the ITO/PPP (d=360 nm)/Al device.

vacuum-deposited poly (p-phenylene) (PPP) thin ilms. The ITO/PPP/Al devices showed an external quantum efficiency of about 0.02 % with an EL emission peak at 446 nm. The onset of the EL occurs at an electric field strength of about 7×10^7 V/m, independent of the thickness of the PPP layer and the temperature. The I-V dependence of all ITO/PPP/Al devices with different PPP thicknesses shows a very weak temperature dependence in the temperature range between 14 and 290 K and fits very well with the FN tunneling formula. The results suggest that charge carrier injection is a tunneling process through an energy barrier of about φ_0 =0.6∼0.8 eV in ITO/PPP/Al.

ACKNOWLEDGMENTS

This work was supported by the Korea Science and Engineering Foundation (KOSEF) through the Quantum-Functional Semiconductor Research Center at Dongguk University.

REFERENCES

[1] J. R. Sheats, H. Antoniadis, M. Hueschen, W. Leonard, J. Miller, R. Moon, D. Roitman and A. Stocking, Science **273**, 884 (1996).

[2] R. H. Friend, R. W. Gymer, A. B. Holmes, J. H. Burroughes, R. N. Marks, C. Taliani, D. D. C. Bradley, D. A. Dos Santos, J. L. Bredas, M. Logdlund and W. R. Salaneck, Nature **397**, 121 (1999).

[3] A. J. Heeger, S. Kivelson, J. R. Schrieffer and W. -P. Su, Rev. Mod. Phys. **60**, 781 (1988).

[4] K. Pakbaz, C. H. Lee, A. J. Heeger, T. Hagler and D. McBranch, Synth. Met. **64**, 295 (1994).

[5] C. H. Lee, J. Y. Park, Y. W. Park, Y. H. Ahn, D. S. Kim, D. H. Hwang and T. Zyung, J. Korean Phys. Soc. **35**, S291 (1999).

[6] C. H. Lee, C. E. Lee and J. I. Jin, J. Korean Phys. Soc. **33**, L532 (1998).

[7] G. Y. Oh and H. Y. Choi, J. Korean Phys. Soc. **32**, 97 (1998).

[8] C. W. Tang and S. A. Van Slyke, Appl. Phys. Lett. **51**, 913 (1987).

[9] I. D. Parker, J. Appl. Phys. **75**, 1656 (1994).

[10] P. S. Davids, Sh. M. Kogan, I. D. Parker and D. L. Smith, Appl. Phys. Lett. **69**, 2270 (1996).

[11] I. H. Campbell, T. W. Hagler, D. L. Smith and J. P. Ferraris, Phys. Rev. Lett. **76**, 1900 (1996).

[12] P. E. Burrows, Z. Shen, V. Bulovic, D. M. McCarty, S. R. Forrest, J. A. Cronin and M. E. Thompson, J. Appl. Phys. **79**, 1991 (1996).

[13] P. W. M. Blom, M. J. M. de Jong and J. J. M. Vleggaar, Appl. Phys. Lett. **68**, 3308 (1996).

[14] A. J. Campbell, D. D. C. Bradley and D. G. Lidzey, J. Appl. Phys. **82**, 6326 (1997).

[15] K. C. Kao and W. Hwang, *Electrical Transport in Solids* (Pergamon Press, Oxford, 1981).

[16] G. Leising, S. Tasch, F. Meghdadi, L. Athouel, G. Froyer and U. Scherf, Synth. Met. **81**, 185 (1996).

[17] K. Miyashita and M. Kaneko, Synth. Met. **68**, 161 (1995).

[18] S. Kobayashi and Y. Haga, Synth. Met. **87**, 31 (1997).

[19] C. H. Lee, G. W. Kang, J. W. Jeon, W. J. Song and C. Seoul, Thin Solid Films **363**, 306 (2000).

[20] W. J. Song, C. Seoul, G. W. Kang and C. H. Lee, Synth. Met. (to be published).

[21] Y. Yang, Q. Pei and A. J. Heeger, J. Appl. Phys. **79**, 934 (1996).

[22] G. W. Kang, C. H. Lee, W. J. Song and C. Seoul, J. Korean Phys. Soc. (to be published).